CORA Cork Open Research Archive
Cartlann Taighde Oscailte Chorcaí

Title	Extreme value estimates using vibration energy harvesting
Authors	Vathakkattil Joseph, George;Hao, Guangbo;Pakrashi, Vikram
Publication date	2018-09-11
Original Citation	Vathakkattil Joseph, G., Hao, G. and Pakrashi, V. (2018) 'Extreme value estimates using vibration energy harvesting', Journal of Sound and Vibration, 437, pp. 29-39. doi:10.1016/j.jsv.2018.08.045
Type of publication	Article (peer-reviewed)
Link to publisher's version	http://www.sciencedirect.com/science/article/pii/S0022460X18305522 - 10.1016/j.jsv.2018.08.045
Rights	© 2018, Elsevier Ltd. All rights reserved. This manuscript version is made available under the CC-BY-NC-ND 4.0 license. - https://creativecommons.org/licenses/by-nc-nd/4.0/
Download date	2026-11-01 22:13:56
Item downloaded from	https://hdl.handle.net/10468/7020



UCC
University College Cork, Ireland
Coláiste na hOllscoile Corcaigh

Extreme Value Estimates using Vibration Energy Harvesting

George Vathakkattil Joseph[a,b,*], Guangbo Hao[c,d], Vikram Pakrashi[a,b]

[a]*Dynamical Systems and Risk Laboratory, University College Dublin*
[b]*Marine and Renewable Energy Ireland (MaREI) Centre, University College Dublin*
[c]*School of Engineering, University College Cork*
[d]*Marine and Renewable Energy Ireland (MaREI) Centre, Environmental Research Institute, University College Cork*

Abstract

This paper establishes the possibility of utilizing energy harvesting from mechanical vibrations to estimate extreme value responses of the host structure and demonstrates the calibration of these estimates for excitation spectra typical to natural systems. For illustrative purposes, a cantilever type energy harvester is considered for wind excitation. The extreme value estimates are established through a Generalized Pareto Distribution (GPD). Classically well-known Kaimal and Davenport spectra for wind have been considered in this paper for comparison purposes. The applicability of GPD for processes with short-range dependence is explored in both linear and nonlinear systems. The work also demonstrates how return levels can be mapped using energy harvesting levels and indicates that vibration energy harvesting, in its own right, has the potential to be used for extreme value analysis and estimates. The work has impact on health monitoring and assessment of built infrastructure in various stages of repair or disrepair and exposed to nature throughout their lifetime.

Keywords: Energy harvesting, Vibration, Extreme value estimation

1. Introduction

Estimation of extreme events and their responses is crucial in designing and engineering structures that can withstand the forces of the physical environment they are subjected to. This is particularly relevant both for ageing built infrastructure[1] burgeoning sectors[2]. The relationship between climate variability or change estimates with those of extreme values[3] makes such estimates more relevant. Estimating the probability of occurrence of severe natural phenomena is of importance to any form of long-term planning. Engineering bridges, dams, sea-walls, off-shore structures, windmills, skyscrapers, etc. are dependent on such estimation and therefore assessment of extreme dynamic responses has been a popular subject of study. The statistical methods of extreme value theory have been developed to facilitate this essential requirement of estimating the probability of extreme levels of a process based on previously observed data. Extreme values are usually characterized by return levels and periods, which are likelihood estimates based on the statistical properties of the processes. There have been numerous studies that condensed empirical data pertaining to several natural phenomena such as wind, ocean waves, and earthquakes to a set of spectra[4, 5, 6, 7, 8], i.e. the power spectral densities (PSD), and the probability distribution functions (PDF), [9, 10, 11, 12, 13], using which the processes can be approximated.

The dynamics of a wide range of structures and their operational conditions can be approximated by using an assumption of linearity and with a single degree of freedom (SDOF) dominating. Recently, with the rise of renewable energy devices (onshore and offshore wind turbines, wave devices, combined wind and wave devices etc.), these structures have become light and more flexible[14]. While this leads to the complexities of nonlinearity or the need to understand more than one degree of freedom, the fundamental basis behind several such existing or conceptual designs at various technological readiness levels are often adequately represented by SDOF systems. This consideration

*Corresponding author
Email address: george.vathakkattiljoseph@ucdconnect.ie (George Vathakkattil Joseph)

highlights the importance of accurate estimation of return periods. New designs can be guided by the estimates of extreme values and this is reflected in their fragility curves. Studying the dynamic responses of the structures to extreme levels can be used to assess structural non-linearities as well[15]. Accurate estimation of the change in extreme value distributions would also contribute to the quantification of change in the operational environment or the system itself.

The accuracy of the estimation relies on having large data-sets, typically over many years, with good resolution. Also, the non-stationary nature of physical phenomena warrants perpetual monitoring of the events, to update the estimates periodically. Conventional methods of measurement like strain gauges, anemometers, inertial measurement units placed in buoys deployed in the ocean, etc,. require power sources to function. This may not be feasible in many cases and a battery may typically require replacement or a solar/wind-powered recharging setup for extending its lifetime for long-term monitoring[16]. Under such circumstances, technologies and methods for extreme value estimates of the responses of the built infrastructure requiring low to no power can be very attractive.

Vibration energy harvesters present themselves as a promising solution for powering such sensors and this has been studied extensively by several groups[17, 18]. Vibration energy harvesters operate by responding to the dynamic response signatures of the host device. For example, dynamic responses of structures can be the base excitation of an energy harvester, which is then converted to voltage through electro-mechanical coupling and a circuit, which may be as simple as a resistor or more complex, based on the requirements of the final application. Under such circumstances, there is an opportunity to use energy harvesters in their own right as monitors. Energy harvesting based structural health monitoring (SHM) has been recently suggested[19, 20]. Such use also reduces instrumentation and helps site-safety in locations where access could be impossible or risk is significant[21]. Another advantage lies in the fact that the magnitude of harvested energy from built infrastructure tends to be small and thus a physical and useful interpretation of its variation, rather than its absolute magnitude, can be more rewarding. In this paper, we demonstrate that the voltage signals generated from a vibration energy harvester subjected to typical natural systems, can be used to estimate extreme value responses of such systems. We show that extreme value responses estimated using inertial data directly correspond to the estimation using voltage signals from the harvester. A recent study[22] has looked at peak-statistics from linear energy harvesters subjected to Gaussian white-noise excitation and derived the probability distribution function of the extremes. This study demonstrates how classical approaches in extreme value theory can be applied to the same as well as broader cases of harvesters and excitation.

2. Conceptual background

The most common approaches to extreme value estimation are based on asymptotic distributions[23]. One approach is to assume that the epochal extremes, such as annual or monthly maxima, are distributed according to the Generalized Extreme Value (GEV) distribution and estimate the parameters of the distribution based on the observed data. This is referred to as the block-maxima approach[23]. A second approach utilizing all available data instead of just sparse maxima is to assume that the values which exceed a threshold follow a Generalized Pareto distribution (GPD) and estimate the model parameters fitting the data[23]. Since we are not theoretically limited in resolution while performing a numerical analysis, and since a better utilization of the data can be made by using the entire time-series[23], we employ the second approach, called the peaks-over-threshold method, for our estimates. Let X denote an arbitrary term in the sequence X_1,X_2,... of independent identically distributed random variables. For a large enough threshold u, the cumulative distribution function of $(X - u)$, conditional on $X > u$, referred to as GPD is:

$$H(X-u) = 1 - \left(1 + \frac{\xi(X-u)}{\sigma}\right)^{-1/\xi} \tag{1}$$

where ξ called the shape parameter and σ as the scale parameter. The parameters can be estimated from the data using the maximum likelihood estimation method[23].

Piezoelectric vibrational energy harvesting has been modelled previously with varying levels of complexity and accuracy[24, 25, 26, 27]. As the intention of this paper is to provide a proof of concept, we settle for a reasonable and established model using the corrected lumped-parameter approach from Erturk and Inman [26]. A cantilever in bi-morph configuration is modelled. The electro-mechanically coupled equations of a linear piezoelectric vibration energy harvester are:

$$m_h\ddot{u} + c_h\dot{u} + k_h u - \theta V = -\mu m_h \ddot{u_b} \tag{2}$$

$$\theta\dot{z} + C_p\dot{V} + \frac{1}{R_l}V = 0 \tag{3}$$

where m_h is the (Rayleigh) equivalent mass of the harvester, c_h is the damping, k_h is the stiffness, u_b is the base excitation of the harvester, u is the tip-displacement of the harvester (u and u_b are along the same direction), θ is the electromechanical coupling coefficient, V is the voltage across the piezoceramic, C_p is the capacitance of the piezoceramic and R_l is the load resistance. μ is a correction factor approximately given by

$$\mu = \frac{(M_t/m)^2 + 0.603(M_t/m) + 0.08955}{(M_t/m)^2 + 0.4637(M_t/m) + 0.05718} \tag{4}$$

where M_t is the tip mass and m is the beam mass of the harvester. The parameters used are given in Table 1.

Natural systems such as ocean-waves, wind, etc., can be approximately represented by specific empirically derived spectra and probability distributions. These can be used to generate a time-series ensemble representing the system. The method of time-series generation is described in Section 3. The probability density function (PDF) of the ensemble can be used to estimate extreme values by fitting the tail of the distribution to a standard extreme value distribution using the approaches described above.

The dynamic response of the structure under analysis, excited by the process represented by the time-series, can be expressed as the output obtained by passing an input signal through a system. Considering the structure to be a linear harmonic oscillator,

$$\ddot{u_b} + 2\zeta_{\text{osc}}\omega_{\text{osc}}\dot{u_b} + {\omega_{\text{osc}}}^2 u_b = F_{\text{ext}}/M_{\text{osc}} \tag{5}$$

where ω_{osc} is the natural frequency, ζ_{osc} is the damping ratio, and M_{osc} is the mass of the SDOF system, we have a second-order linear system through which the excitation time-series, F_{ext}, representing a realization of the process, is passed through. Since the structure hosts the energy harvester, the acceleration of the structure acts as the base acceleration of the harvester (ref Fig. 1). In the case of a harvester excited by a linear stochastic process, the power spectral density(PSD) of the base acceleration, $S_a(\omega)$, is related to the PSD of the harvester voltage, $S_v(\omega)$, through the voltage frequency response function (FRF) $\alpha(\omega)$ obtained from harmonic excitation[28]

$$S_v(\omega) = |\alpha(\omega)|^2 S_a(\omega) \tag{6}$$

Thus we have a linear system again between the acceleration from the host structure and the harvester output. Since the cascaded transformations are linear, the cumulative distribution function (CDF) of the voltage generated can be mapped to the CDF of the base-acceleration of the harvester and also to the CDF of the excitation process. This establishes that any extreme value estimation done purely based on the spectra, or through the data obtained from a traditional inertial sensor can be done with the same approach and confidence level using an energy harvester, once calibrated. Adhikari et al.[22] has shown that the fractional occupation time above a threshold for a linear harvester excited by white Gaussian noise can be modelled as a complementary error function(erfc). The erfc can be numerically shown to be closely fitted using a Generalized Pareto PDF. We further explore the cases of weakly nonlinear host structure and nonlinear harvester to discuss the applicability of the GPD in such cases. In cases where an appropriate extreme value distribution can be fitted, linear or nonlinear, we show that a one-to-one mapping of the return levels can be derived.

3. Numerical Formulation

A numerical experiment was carried out to estimate extreme values based on a) the excitation time-series, b) acceleration of the structure, and c) voltage generated by the harvester, which were then compared. As a benchmark analysis, the host structure was excited using Gaussian white noise as the forcing function. To demonstrate the applicability in a practical scenario, wind acting on a structure was simulated. An ensemble of time-series generated

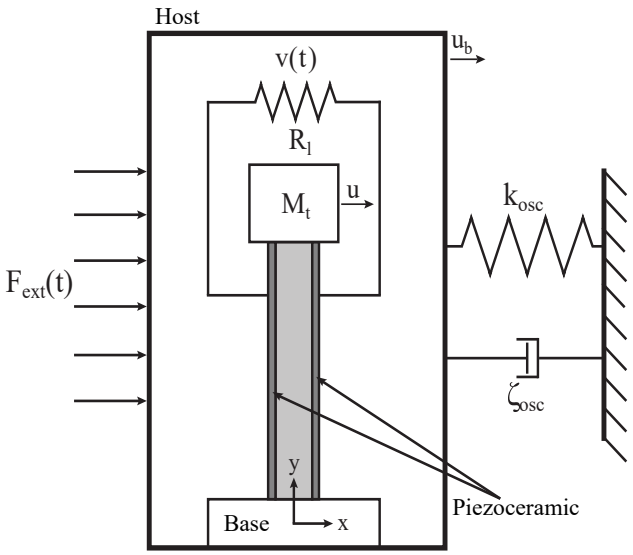


Figure 1: Schematic of the harvester system

randomly based on the theory mentioned above, captures the statistics of the process and extreme value theory can be applied to the combined dataset.

For Gaussian white noise, a time-series of power 10 dBW was generated. The wind-speed time series has a low-frequency component approximated by a Weibull distribution and a high-frequency component approximated by the classical Kaimal and Davenport spectra. 10-minute averages of wind-speed were generated using the Weibull distribution and turbulence signals based on the inverse Fourier transform of the spectra were added at a sampling frequency of 25 Hz. The low-frequency component, ie. 10-minute mean speeds are uncorrelated.

The turbulence spectra are defined for a given mean wind speed $V(z)$ at a given height z. The Kaimal spectrum[7] is expressed as:

$$\frac{nS(n)}{v_f^2} = \frac{105f}{(1+33f)^{5/3}} \tag{7}$$

where n is the frequency in Hertz, $S(n)$ is the PSD of wind speed fluctuations, f is the normalised frequency $nz/V(z)$, and v_f is the friction velocity given by

$$u_f = \frac{kV(z)}{ln(z/z_0)} \tag{8}$$

where k is the von Karman's constant ($k = 0.4$) and z_0 is the reference height ($z_0 = 0.025$). The Davenport spectrum[8] is expressed as:

$$\frac{nS(n)}{v_f^2} = \frac{4x^2}{(1+x^2)^{4/3}} \tag{9}$$

where $x = 1200f/z$. The wind velocity time series is used to calculate pressure by utilizing the simple relation

$$p = \frac{1}{2} \times \text{density of air} \times \text{wind velocity}^2 \times \text{shape factor} \tag{10}$$

where the density of air is taken as 1.25 and shape factor as unity. Force is calculated by multiplying with unit area. The force acts upon the host structure and thus the force time series is applied to a harmonic SDOF oscillator whose parameters are listed in Table 1. The energy harvester is attached to the host structure at its base, thereby making the base acceleration of the harvester the same as the acceleration of the SDOF oscillator. The parameters of the harvester(from [19]) are listed in Table 1. The second order equation for the SDOF oscillator and the coupled

Parameter	Symbol	Value	Unit
SDOF oscillator			
Mass	M_{osc}	1	kg
Damping ratio	ζ_{osc}	0.02148	
Natural frequency	ω_{osc}	12.79	Hz
Harvester			
Tip mass	M_t	0.03	kg
Beam mass	m	0.01365	kg
Damping ratio	$c_h/2\sqrt{k_h m_h}$	0.04	
Load resistance	R_l	1000000	Ω
Capacitance of piezoceramic	C_p	1.966	nF
Natural frequency	$\sqrt{k_h/m_h}$	12.79	Hz
Electromechanical coupling	θ	1.289	μC/m

Table 1: Harvester and oscillator parameters

equations for the harvester are solved at the two stages based on an explicit Runge-Kutta (4,5) scheme, the Dormand-Prince pair[29]. The time-series is generated at a sampling frequency of 25Hz for a duration of 3600s leading to 90,000 points per series. An ensemble of 100 series is generated for each spectrum. After obtaining the time-series of the wind-speed, the acceleration, and the voltage, we proceed to estimate extreme values using each data-set. This process is repeated for (a) linear harvester attached to a host structure with weak-nonlinearity and (b) nonlinear harvester attached to a linear host. In both cases, a cubic nonlinearity was added where the coefficient of the cubic term was 1/10-th of the linear term.

In order to fit a GPD model, an appropriate threshold choice should be made. A reasonably high threshold can be chosen in many cases from physical interpretation of the data. A practical engineering approach to choose a threshold would be to look at the empirical CDF of the data and choose a high enough threshold below the required percentile. The percentiles above which extremes are to be estimated are generally above the 95th percentile, which corresponds to a CDF value of 0.95. We have considered the magnitude of acceleration and voltage as it is often more important for dynamic responses. Using the value at CDF = 0.95 as the threshold, we proceed to fit the distribution using the maximum likelihood estimation method and find the model parameters.

A fundamental condition of the extreme value theorem on which the theory is based is that the random variables are independent and identically distributed (iid). The utilization of a non-white spectrum to describe the high-frequency component of the wind-speed makes the random variables non-independent, ie. autocorrelation exists. This would *prima facie* mean that the GPD cannot be applied to the time-series. However, we observe from the results that this is not the case always. We attempt to explain this using the nature of the correlograms.

4. Results

4.1. GPD fit

The thresholds used and the model parameters obtained for each time-series are listed in Table 2. The data is trimmed by 10 seconds at the beginning to avoid transients. For the white-noise excitation, the harvester voltage levels show good agreement with the results derived in [28]. Probability plots (Q-Q plots with modified axes) showing goodness of fit of the white-noise excited case is given in Figure 2. The quantiles of the GPD fit is plotted against the simulated time-series. Coinciding plots indicate a perfect match between the dataset and the fitted distribution. In the white-noise excited case, the graphs are coincident across most of the plot showing the validity of using the GP distribution and the estimation method we adopted. A Q-Q plot magnifies deviations at the extremes compared to the lower quantiles. Coincident plots at higher values reflect excellent agreement of the fit with the dataset.

Figures 3,4,5,6,7,8 correspond to the wind-spectra. The linear and nonlinear cases for both spectra are shown. It may be noted here that the token threshold choice of 0.95 can be altered for a better fit as required by the estimation case and guided by the threshold selection constraints imposed by the data [23].

Parameters	Linear		Nonlinear host		Nonlinear harvester	
	Kaimal	Davenport	Kaimal	Davenport	Kaimal	Davenport
Threshold						
Wind-speed (ms^{-1})	15.392	15.707	15.292	15.796	15.317	15.786
Acceleration (ms^{-2})	8.802	6.801	8.772	6.841	8.775	6.824
Voltage (V)	1.147	0.889	1.143	0.894	1.144	0.892
GPD fit						
Shape parameter - Wind-speed	-0.183	-0.134	-0.176	-0.135	-0.182	-0.134
Shape parameter - Acceleration	-0.001	0.054	0.001	0.056	0.0005	0.053
Shape parameter - Voltage	-0.004	0.052	-0.005	0.054	-0.005	0.050
Scale parameter - Wind-speed	2.625	2.440	2.565	2.462	2.637	2.444
Scale parameter - Acceleration	3.103	2.264	3.084	2.287	3.092	2.277
Scale parameter - Voltage	0.407	0.296	0.404	0.299	0.405	0.298

Table 2: Thresholds and fitted model parameters

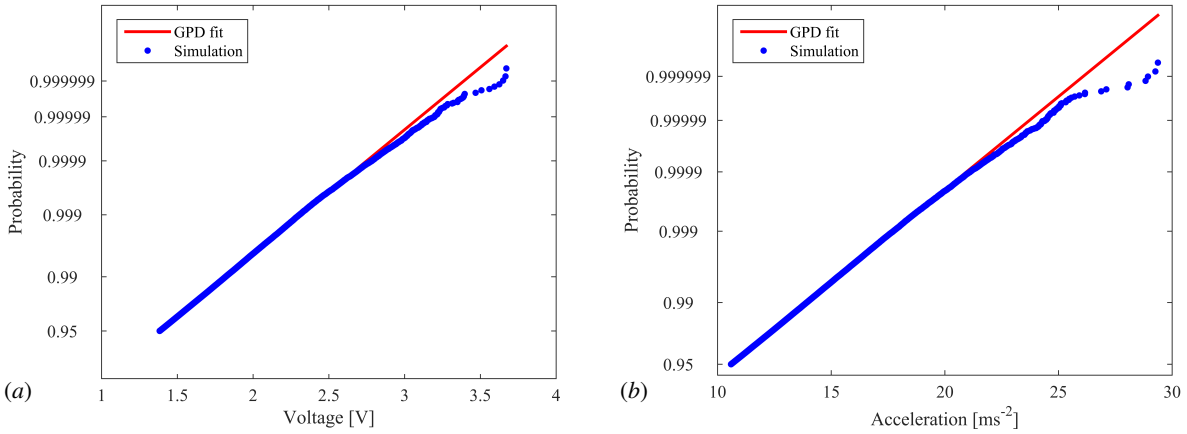


Figure 2: Probability plots of (a)Voltage from harvester, (b)Acceleration of host structure from Gaussian white noise excitation

Time-series from the Kaimal spectrum show a very good agreement for all cases. Time-series from the Davenport spectrum appear to fit well up to a probability level of 0.9999 and then deviate from the GP fit.

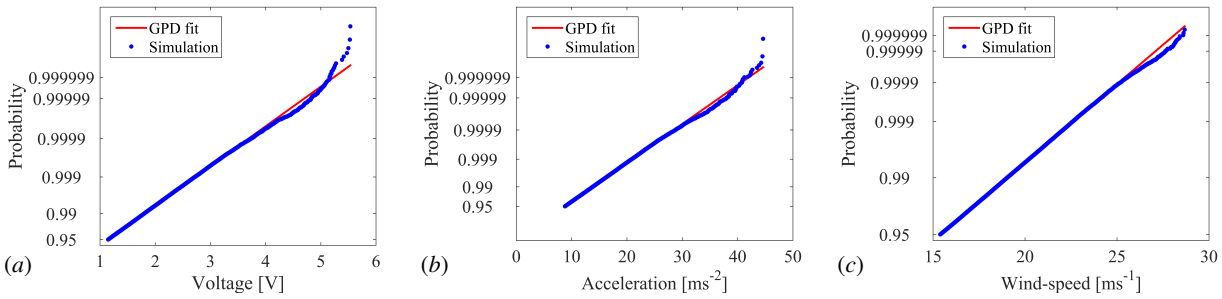


Figure 3: Probability plots of (a)Voltage from harvester, (b)Acceleration of host structure, and (c)Wind-speed from Kaimal spectrum excitation on linear host with linear harvester

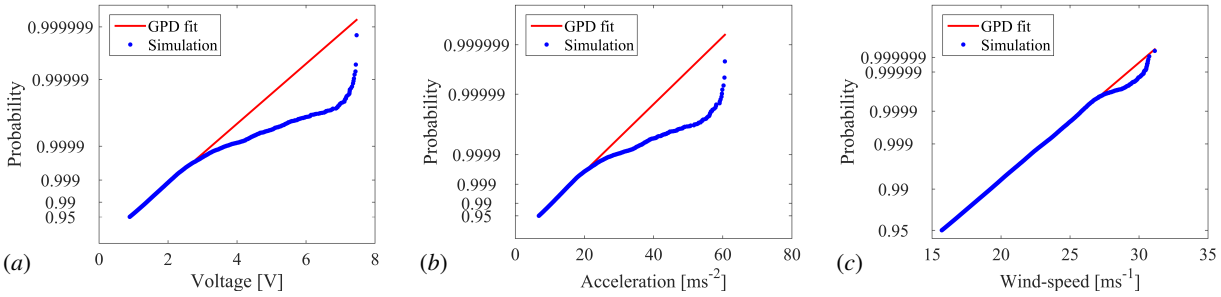


Figure 4: Probability plots of (a)Voltage from harvester, (b)Acceleration of host structure, and (c)Wind-speed from Davenport spectrum excitation on linear host with linear harvester

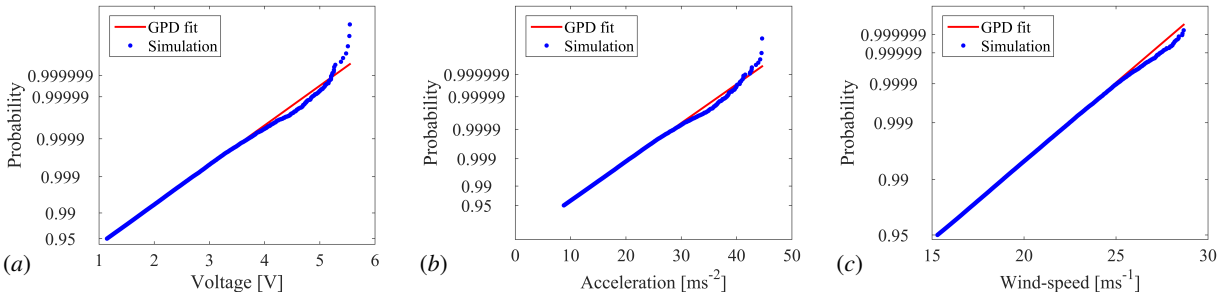


Figure 5: Probability plots of (a)Voltage from harvester, (b)Acceleration of host structure, and (c)Wind-speed from Kaimal spectrum excitation on nonlinear host with linear harvester

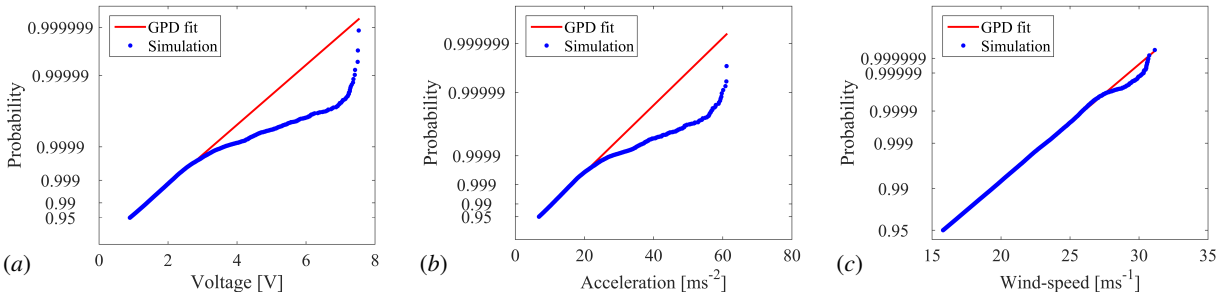


Figure 6: Probability plots of (a)Voltage from harvester, (b)Acceleration of host structure, and (c)Wind-speed from Davenport spectrum excitation on nonlinear host with linear harvester

4.2. Analysis of dependence

An analysis of the impact of short-range dependence on extremes[30] provides a result that rare-events that are sufficiently separated can be treated as almost independent. 'Sufficient' implied here is relatively small. In the wind-speed time-series, the 10-minute mean-speeds are independent. The turbulence within the 10 minute (600s) window can be considered to be dependent in the short-range. The correlograms(Figs.9,12) of the wind-speed time-series also show that the perfect correlation in the short-range falls to near-zero after 600s.

Passing the force due to the wind-speed through the host structure and the harvester appears to decrease the correlation even for the short-range (Figs.10,11,13,14), allowing an assumption of near-independence for the ensemble. Similar to the wind-speed series, this explains the good fit obtained in multiple cases. The deviation of the Davenport-excited cases from the fitted distribution can also be explained using the higher auto-correlation levels in those situations(Fig.15). Intuitively, the higher PSD levels of the Davenport spectrum lead to stronger gusts, thereby making rare-events closer than in the Kaimal case. Therefore, at probability levels that are significantly high (in this

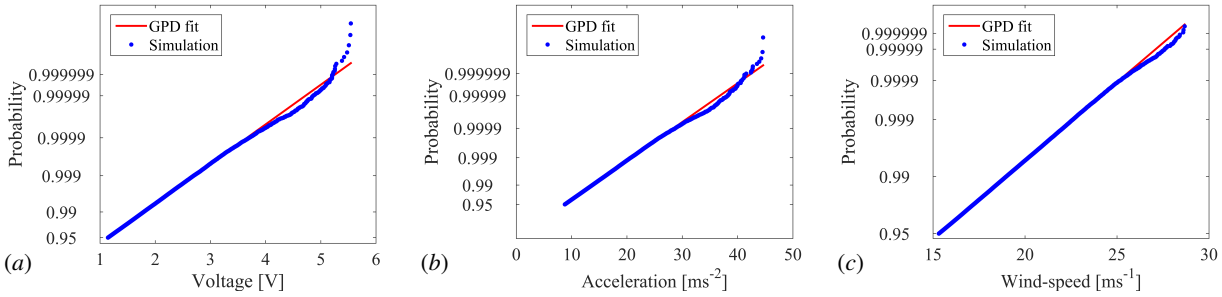


Figure 7: Probability plots of (a)Voltage from harvester, (b)Acceleration of host structure, and (c)Wind-speed from Kaimal spectrum excitation on linear host with nonlinear harvester

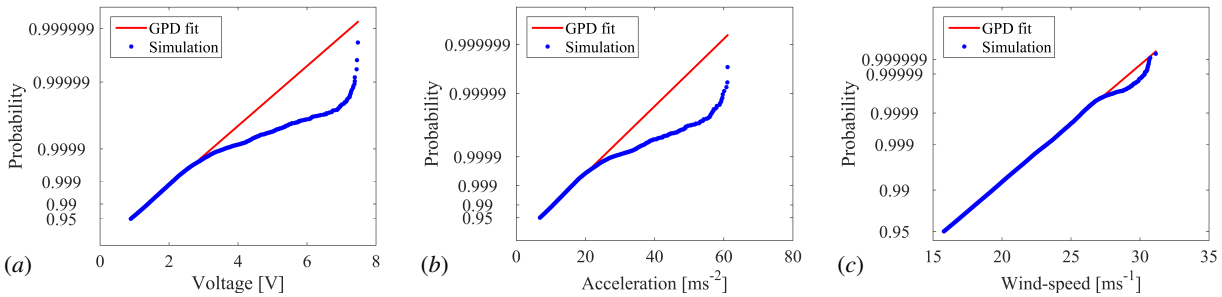


Figure 8: Probability plots of (a)Voltage from harvester, (b)Acceleration of host structure, and (c)Wind-speed from Davenport spectrum excitation on linear host with nonlinear harvester

case, above approx. 0.9999), the data shows more occurrences of rare events than predicted by the EV distribution. Figure 15a) and 15b) show higher levels of auto-correlation of voltage/acceleration for Davenport excitation which in turn leads to a poor fit, whereas figure 15c) shows that the auto-correlation levels of Davenport wind-speed are about the same as Kaimal, leading to a good fit as observed in Figs.4(c),6(c),8(c). (Auto-correlation values from lag = 700s to 3599s were used to calculate the root-mean-square averages in each iteration). The correlograms and the RMS autocorrelation plots are similar for nonlinear cases. They are excluded for brevity. For a rigorous treatment of EV theory applied to data with short-range dependence, the reader may peruse Ref.[30] and the references therein.

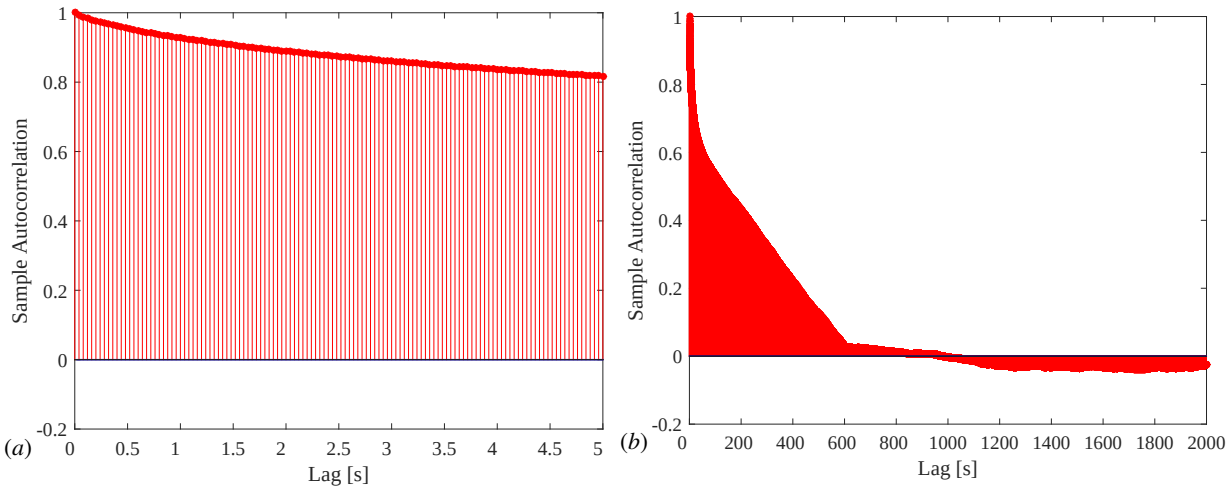


Figure 9: Correlograms for Kaimal wind-speeds. (a)Lag upto 5 seconds, (b)Lag upto 2000 seconds

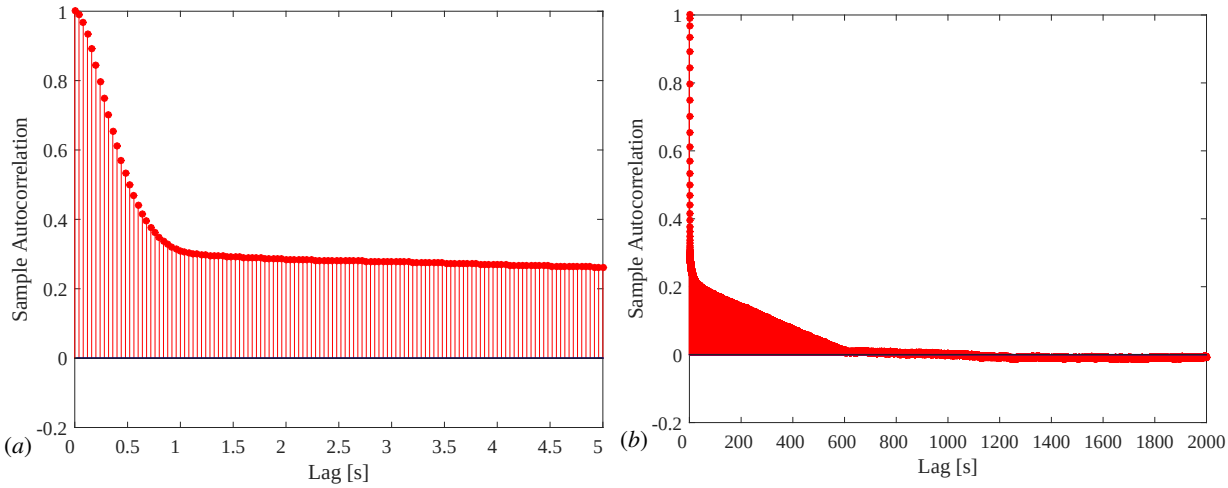


Figure 10: Correlograms for acceleration due to Kaimal excitation. (a)Lag upto 5 seconds, (b)Lag upto 2000 seconds

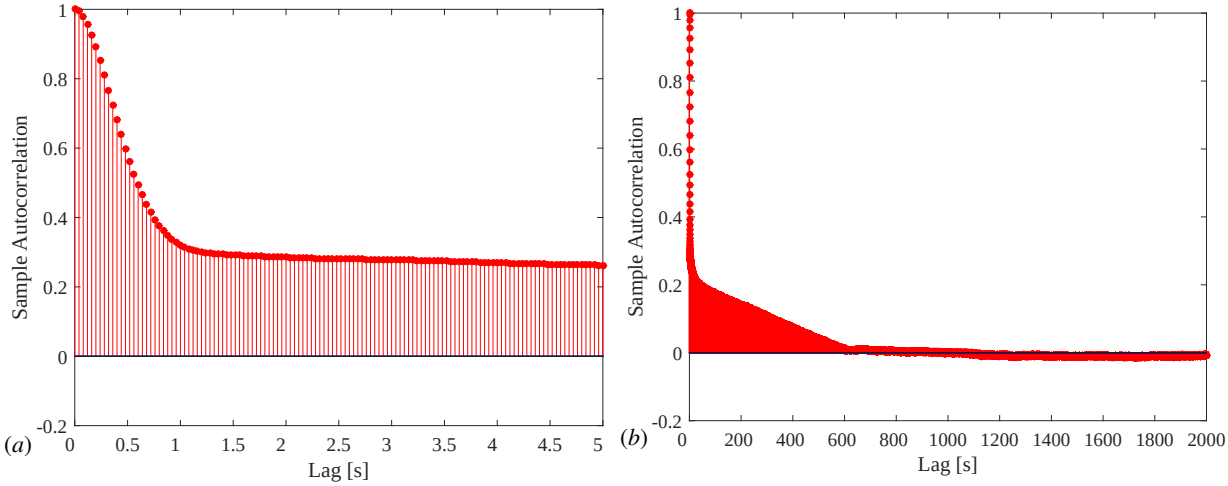


Figure 11: Correlograms for voltage due to Kaimal excitation. (a)Lag upto 5 seconds, (b)Lag upto 2000 seconds

4.3. Return level estimation

We now proceed to estimate the return levels from our modelled distributions. Our objective is to estimate the return level of a, say, 100-year wind event and map them to a corresponding voltage level. We demonstrate that such a mapping can be achieved by relating the fitted distributions of wind-speed, acceleration, and voltage by a statistical calibration. However, since our data is non-independent, the interpretation of such return levels should be done with care as clustering could occur. On average a 100-year event would occur ten times in a millennium, but all ten events could tend to be clustered together leading to a significantly lesser chance of their occurrence in the rest of the millennium. Such considerations could be highly relevant for structural design[30].

Assuming that the GPD can be used to fit the data, the probability can be expressed as 1−(CDF), i.e.

$$Pr(X > x \,|\, X > u) = \left[1 + \frac{\xi(x-u)}{\sigma}\right]^{-1/\xi} \tag{11}$$

Using Bayes theorem,

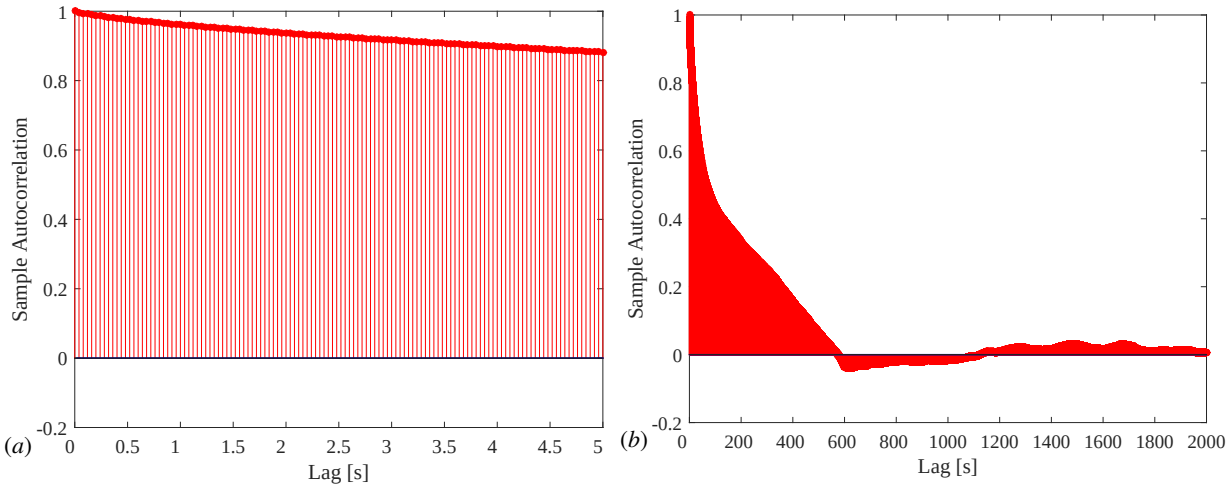


Figure 12: Correlograms for Davenport wind-speeds. (a)Lag upto 5 seconds, (b)Lag upto 2000 seconds

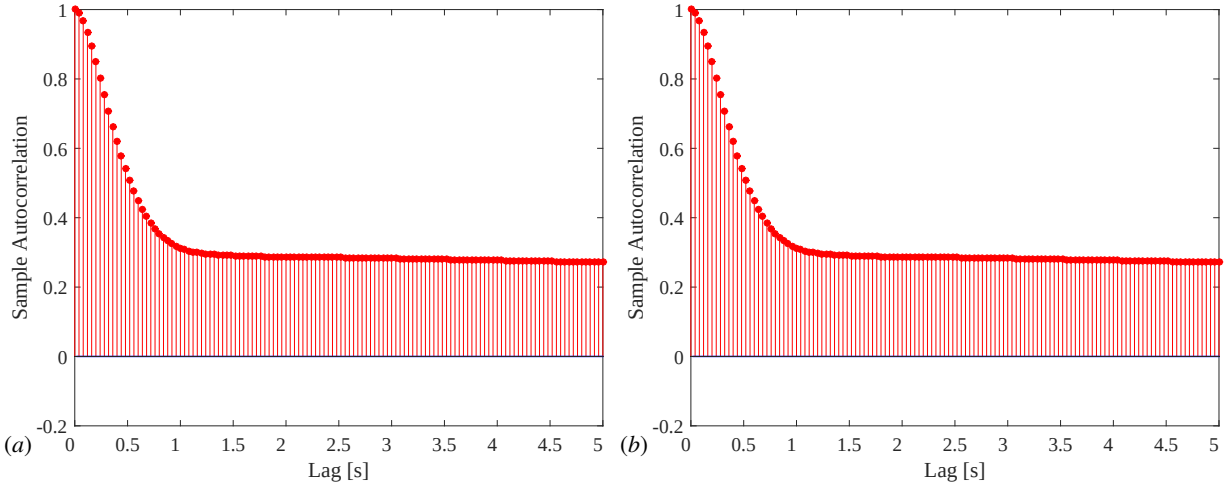


Figure 13: Correlograms for acceleration due to Davenport excitation. (a)Lag upto 5 seconds, (b)Lag upto 2000 seconds

$$\begin{aligned} Pr(X > x) &= Pr(X > u)\left[1 + \frac{\xi y}{\sigma}\right]^{-1/\xi} \\ &= \lambda\left[1 + \frac{\xi(x-u)}{\sigma}\right]^{-1/\xi} \end{aligned} \tag{12}$$

where λ is the empirical threshold exceedance probability, i.e. the fraction of samples above the chosen threshold. Thus, an estimate of the level z that is exceeded on average once every t observations is obtained by solving

$$Pr(X > z) = \lambda\left[1 + \frac{\xi(z-u)}{\sigma}\right]^{-1/\xi} = \frac{1}{t} \tag{13}$$

Rearranging for z,

$$z = u + \frac{\sigma}{\xi}\Big[(t\lambda)^{\xi} - 1\Big] \tag{14}$$

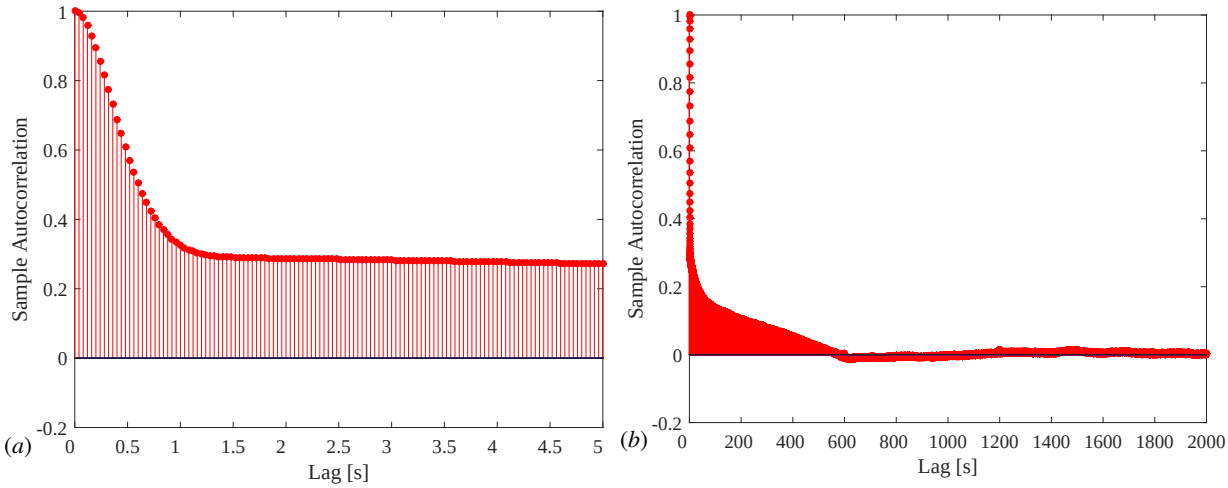


Figure 14: Correlograms for voltage due to Davenport excitation. (a)Lag upto 5 seconds, (b)Lag upto 2000 seconds

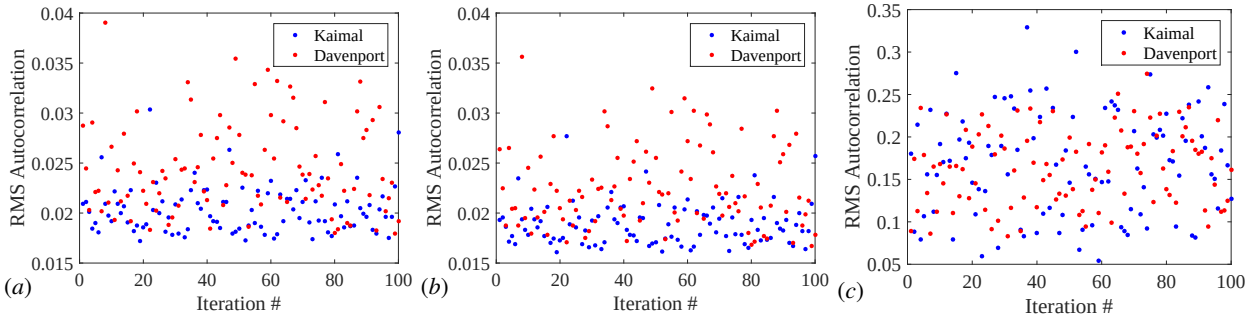


Figure 15: RMS autocorrelation (a)Voltage, (b)Acceleration, (c)Wind-speed

z is the t-observation return level. If there are n observations per year, then the r-year return level can be expressed as

$$z = u + \frac{\sigma}{\xi}\Big[(rn\lambda)^{\xi} - 1\Big] \tag{15}$$

For the same sampling rate, the number of observations t and consequently Eq. 13 should be equal for wind-speed, acceleration and voltage. i.e.,

$$\lambda_w\left[1 + \frac{\xi_w(z_w - u_w)}{\sigma_w}\right]^{-1/\xi_w} = \lambda_a\left[1 + \frac{\xi_a(z_a - u_a)}{\sigma_a}\right]^{-1/\xi_a} = \lambda_v\left[1 + \frac{\xi_v(z_v - u_v)}{\sigma_v}\right]^{-1/\xi_v} \tag{16}$$

Using the same λ for all three data-sets gives us the mapping between the return levels as:

$$\left[1 + \frac{\xi_w(z_w - u_w)}{\sigma_w}\right]^{-1/\xi_w} = \left[1 + \frac{\xi_a(z_a - u_a)}{\sigma_a}\right]^{-1/\xi_a} = \left[1 + \frac{\xi_v(z_v - u_v)}{\sigma_v}\right]^{-1/\xi_v} \tag{17}$$

Once calibrated using an appropriate GPD model, the return levels of the acceleration(z_a; Eq.18) of the host structure, and wind-speed(z_w; Eq.19) can be expressed as functions of the return level of voltage(z_v). Figures 16,17,18 show the mapping based on the fit obtained above.

$$z_a = u_a + \frac{\sigma_a}{\xi_a}\left[\left(1 + \frac{\xi_v(z_v - u_v)}{\sigma_v}\right)^{\frac{\xi_a}{\xi_v}} - 1\right] \tag{18}$$

$$z_w = u_w + \frac{\sigma_w}{\xi_w}\left[\left(1 + \frac{\xi_v(z_v - u_v)}{\sigma_v}\right)^{\frac{\xi_w}{\xi_v}} - 1\right] \tag{19}$$

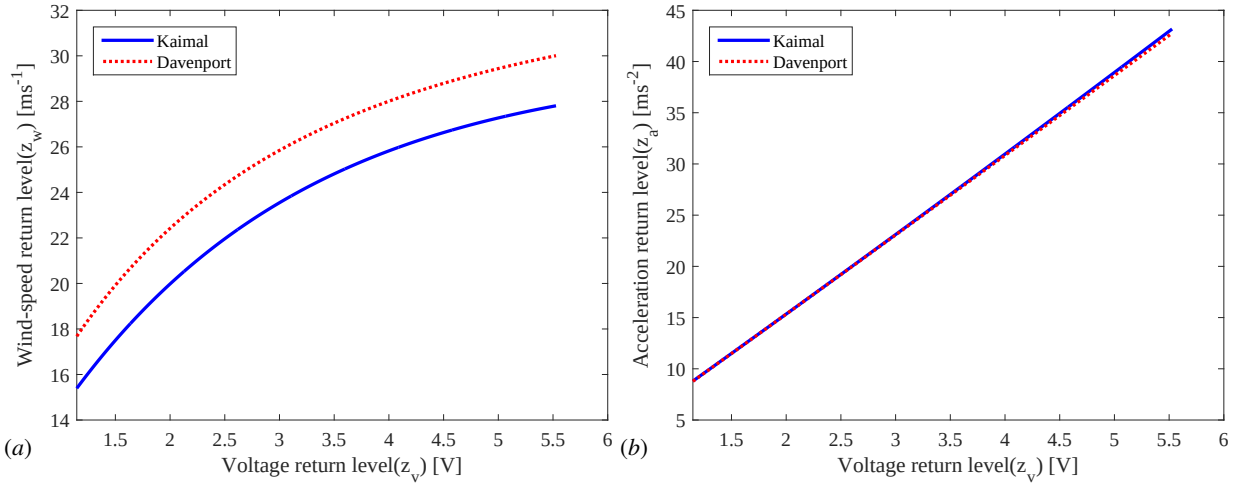


Figure 16: Return level mapping for linear system (a)Wind-speed (b)Acceleration

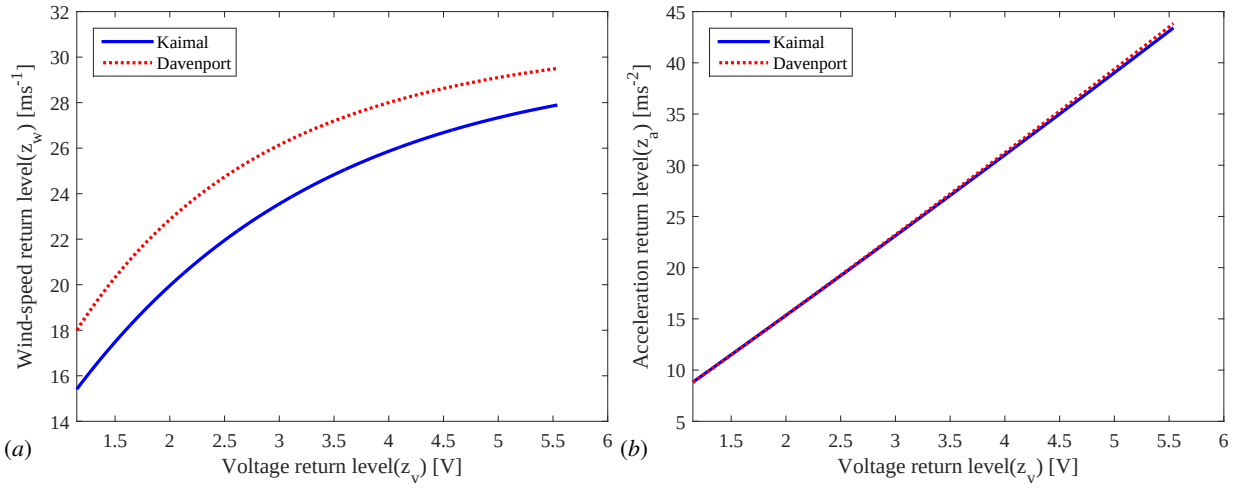


Figure 17: Return level mapping for nonlinear host system (a)Wind-speed (b)Acceleration

The number of iterations employed and thereby the size of the data-set is relatively small compared to data sets sometimes used for extreme-value analysis [31, 32]. An increase in the number of iterations in this study appears to only benefit towards improved proximity to the convergent asymptotic values. Occurrences of higher-magnitude extreme events, if any, in further iterations/durations can be considered as independent events, and as a result EV theory would naturally be valid.

5. Conclusions

This paper has established how analysis of harvested energy from vibrations of structures can be used to estimate extreme value responses and related return periods. The study complements analyses of peak-statistics of energy harvesters done elsewhere in the literature by demonstrating that standard probability distributions from extreme

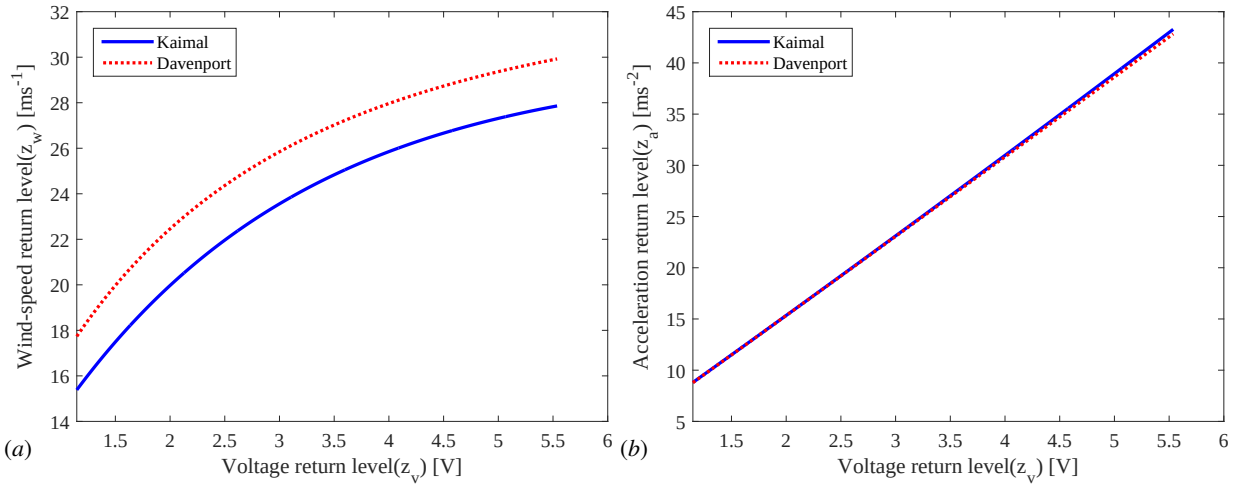


Figure 18: Return level mapping for nonlinear harvester system (a)Wind-speed (b)Acceleration

value theory may be used in a range of cases thereby simplifying analysis. A cantilever-style piezoelectric harvester connected to an SDOF host was considered in this regard, excited by wind loading derived from Kaimal and Davenport spectra respectively, in addition to Gaussian white noise excitation. The extremes were fitted with an asymptotic Generalized Pareto Distribution using maximum likelihood estimation. Applicability of extreme value theory despite short-range dependence in the data is demonstrated. Good fits were obtained for moderate turbulence and also for weakly nonlinear host and harvester despite non-trivial auto-correlation up to 10 minutes. For stronger turbulence, the fit appears to deviate after a probability level of approximately 0.9999. The goodness of fit allows the usage of the established extreme value theory without resorting to advanced analytical or time-series methods. The existence of a return level mapping between the different quantities of interest was shown and the relation was derived. The mapping allows voltage data from the harvester to be directly used for extreme value prediction thereby reducing system complexity and extending the capabilities of energy harvesters as monitors of built infrastructure. The results may also be useful to ascertain the fragility curves of the host structure.

Acknowledgements

The authors would like to acknowledge J.N. Tata Endowment and Marine and Renewable Energy Ireland (MaREI), grant no. 12/RC/2302, a Science Foundation Ireland (SFI) supported project.

[1] A. Znidaric, V. Pakrashi, E. J. O'Brien, et al., A review of road structure data in six european countries, Proceedings of the ICE-Journal of Urban Design and Planning 164 (4) (2011) 225–232.
[2] A. Quilligan, A. OConnor, V. Pakrashi, Fragility analysis of steel and concrete wind turbine towers, Engineering structures 36 (2012) 270–282.
[3] D. Cooley, Extreme value analysis and the study of climate change, Climatic change 97 (1) (2009) 77–83.
[4] W. J. Pierson, L. Moskowitz, A proposed spectral form for fully developed wind seas based on the similarity theory of SA Kitaigorodskii, Journal of geophysical research 69 (24) (1964) 5181–5190.
[5] T. Elfouhaily, B. Chapron, K. Katsaros, D. Vandemark, A unified directional spectrum for long and short wind-driven waves, Journal of Geophysical Research: Oceans 102 (C7) (1997) 15781–15796.
[6] J. N. Brune, Tectonic stress and the spectra of seismic shear waves from earthquakes, Journal of geophysical research 75 (26) (1970) 4997–5009.
[7] J. C. Kaimal, J. Wyngaard, Y. Izumi, O. Coté, Spectral characteristics of surface-layer turbulence, Quarterly Journal of the Royal Meteorological Society 98 (417) (1972) 563–589.
[8] A. G. Davenport, The spectrum of horizontal gustiness near the ground in high winds, Quarterly Journal of the Royal Meteorological Society 87 (372) (1961) 194–211.
[9] E. C. Morgan, M. Lackner, R. M. Vogel, L. G. Baise, Probability distributions for offshore wind speeds, Energy Conversion and Management 52 (1) (2011) 15–26.
[10] J. A. Carta, P. Ramirez, S. Velazquez, A review of wind speed probability distributions used in wind energy analysis: Case studies in the canary islands, Renewable and Sustainable Energy Reviews 13 (5) (2009) 933–955.

[11] N. E. Huang, S. R. Long, An experimental study of the surface elevation probability distribution and statistics of wind-generated waves, Journal of Fluid Mechanics 101 (1) (1980) 179–200.
[12] E. B. Thornton, R. Guza, Transformation of wave height distribution, Journal of Geophysical Research: Oceans 88 (C10) (1983) 5925–5938.
[13] G. Z. Forristall, On the statistical distribution of wave heights in a storm, Journal of Geophysical Research: Oceans 83 (C5) (1978) 2353–2358.
[14] J. Arrigan, V. Pakrashi, B. Basu, S. Nagarajaiah, Control of flapwise vibrations in wind turbine blades using semi-active tuned mass dampers, Structural Control and Health Monitoring 18 (8) (2011) 840–851.
[15] V. Pakrashi, P. Fitzgerald, M. OLeary, V. Jaksic, K. Ryan, B. Basu, Assessment of structural nonlinearities employing extremes of dynamic responses, Journal of Vibration and Control (2016) 1077546316635935.
[16] A. Dewan, S. U. Ay, M. N. Karim, H. Beyenal, Alternative power sources for remote sensors: A review, Journal of power sources 245 (2014) 129–143.
[17] H. Li, C. Tian, Z. D. Deng, Energy harvesting from low frequency applications using piezoelectric materials, Applied physics reviews 1 (4) (2014) 041301.
[18] A. R. M. Siddique, S. Mahmud, B. Van Heyst, A comprehensive review on vibration based micro power generators using electromagnetic and piezoelectric transducer mechanisms, Energy Conversion and Management 106 (2015) 728–747.
[19] P. Cahill, V. Jaksic, J. Keane, A. O'Sullivan, A. Mathewson, S. F. Ali, V. Pakrashi, Effect of road surface, vehicle, and device characteristics on energy harvesting from bridge–vehicle interactions, Computer-Aided Civil and Infrastructure Engineering 31 (12) (2016) 921–935.
[20] P. Cahill, N. A. N. Nuallain, N. Jackson, A. Mathewson, R. Karoumi, V. Pakrashi, Energy harvesting from train-induced response in bridges, Journal of Bridge Engineering 19 (9) (2014) 04014034.
[21] V. Pakrashi, J. Harkin, J. Kelly, A. Farrell, S. Nanukuttan, Monitoring and repair of an impact damaged prestressed bridge, Proceedings of the ICE-Bridge Engineering 166 (1) (2012) 16–29.
[22] S. Adhikari, M. Friswell, G. Litak, H. H. Khodaparast, Design and analysis of vibration energy harvesters based on peak response statistics, Smart Materials and Structures 25 (6) (2016) 065009.
[23] S. Coles, J. Bawa, L. Trenner, P. Dorazio, An introduction to statistical modeling of extreme values, Vol. 208, Springer, 2001.
[24] C. Williams, R. B. Yates, Analysis of a micro-electric generator for microsystems, Sensors and Actuators A: Physical 52 (1-3) (1996) 8–11.
[25] N. E. Dutoit, B. L. Wardle, S.-G. Kim, Design considerations for mems-scale piezoelectric mechanical vibration energy harvesters, Integrated Ferroelectrics 71 (1) (2005) 121–160.
[26] A. Erturk, D. J. Inman, On mechanical modeling of cantilevered piezoelectric vibration energy harvesters, Journal of Intelligent Material Systems and Structures 19 (11) (2008) 1311–1325.
[27] A. Erturk, D. J. Inman, A distributed parameter electromechanical model for cantilevered piezoelectric energy harvesters, Journal of vibration and acoustics 130 (4) (2008) 041002.
[28] A. Erturk, D. J. Inman, Piezoelectric energy harvesting, John Wiley & Sons, 2011.
[29] J. R. Dormand, P. J. Prince, A family of embedded runge-kutta formulae, Journal of computational and applied mathematics 6 (1) (1980) 19–26.
[30] V. Chavez-Demoulin, A. Davison, Modelling time series extremes, REVSTAT-Statistical Journal 10 (EPFL-ARTICLE-180506) (2012) 109–133.
[31] A. Naess, Estimation of long return period design values for wind speeds, Journal of Engineering Mechanics 124 (3) (1998) 252–259.
[32] S. Caires, A. Sterl, 100-year return value estimates for ocean wind speed and significant wave height from the era-40 data, Journal of Climate 18 (7) (2005) 1032–1048.